

FSQP nuclear matrix elements for two neutrino double beta decays

H. Ejiri

1. Research Center for Nuclear Physics, Osaka University, Ibaraki, Osaka, 567-0047, Japan

E-mail: ejiri@rcnp.osaka-u.ac.jp

Abstract. Nuclear matrix elements (NMEs $M^{2\nu}$) for two neutrino double beta decays (DBDs) are discussed in terms of the Fermi Surface Quasi Particle model (FSQP). The NMEs for $0^+ \leftrightarrow 0^+$ ground-state-to-ground-state DBDs depend on the Fermi surface shell configuration and the nuclear core polarization. The evaluated NMEs $M^{2\nu}(FSQP)$ reproduce well the observed NMEs $M^{2\nu}(EXP)$ for $2\nu\beta^-\beta^-$ decays. The NMEs $M^{2\nu}(FSQP)$ for the 2ν DBDs of ^{78}Kr , ^{106}Cd and ^{130}Ba and ^{110}Pd are evaluated on the basis of FSQP. The dependence of $M^{2\nu}(FSQP)$ and $M^{2\nu}(EXP)$ on the shell configuration is found to be seen in theoretical NMEs for neutrinoless DBDs. Impacts of $M^{2\nu}(FSQP)$ on $0\nu\beta\beta$ NMEs and $0\nu\beta\beta$ experiments are discussed.

Key words: Double beta decay, two neutrino double beta decay, nuclear matrix element, Fermi surface quasi particle model, shell configuration.

1. Introduction

Neutrino-less double beta decays ($0\nu\beta\beta$), which are beyond the standard electro-weak model (SM), are unique probes for studying the Majorana nature of neutrinos (ν), the absolute ν -mass scales, and others beyond SM. Nuclear matrix elements (NMEs) $M^{0\nu}$ for $0\nu\beta\beta$ are crucial to extract neutrino properties from double beta decay (DBD) experiments, and even to design DBD detectors since the detector sensitivity depends much on $M^{0\nu}$. They are discussed in recent review articles [1, 2, 3, 4, 5] and references therein.

At present, the $0\nu\beta\beta$ rates and the ν -mass are not known experimentally, and thus $M^{0\nu}$ is not known experimentally. On the other hand, two neutrino double beta decays ($2\nu\beta\beta$), which are within SM, are measured experimentally for $2\beta^-$ DBD nuclei of current interests, and thus NMEs $M^{2\nu}$ for them are known experimentally.

Extensive theoretical works have been made on $M^{0\nu}$ and $M^{2\nu}$. Actually they are very small and sensitive to nucleonic and non-nucleonic nuclear correlations, nuclear models and nuclear structures [2, 6, 7, 8, 9]. Therefore accurate theoretical calculations for $M^{0\nu}$ and $M^{2\nu}$ are very hard.

Recently, the Fermi Surface Quasi Particle model (FSQP) based on experimental single- β NMEs M^\pm for low-lying (fermi surface) quasi-particle states is shown to reproduce well $M^{2\nu}(\text{EXP})$ for $\beta^-\beta^-$ decays extracted from the observed $2\nu\beta^-\beta^-$ decay rates. No experimental rates are known for $2\nu\text{ECEC}$, $2\nu\beta^+\text{EC}$ and $2\nu\beta^+\beta^+$ decays, except a geochemical experiment for ^{130}Ba [10]. In fact, it is widely believed that the 2ν and 0ν DBD nuclear processes are so different that their NMEs of $M^{2\nu}$ and $M^{0\nu}$ are independent of each other.

The purpose of the present paper is to study the nuclear structure dependence of the FSQP NMEs $M^{2\nu}(\text{FSQP})$, and to evaluate the NMEs $M^{2\nu}$ for several $2\nu\beta^-\beta^-$ and $2\nu\text{ECEC}$, $2\nu\beta^+\text{EC}$, $2\nu\beta^+\beta^+$ decays of current interest. Then we discuss possible nuclear structure effects on $0\nu\beta\beta$ $M^{0\nu}$ on the basis of FSQP to see if the 2ν NMEs and 0ν DBD NMEs have some common features.

2. Fermi surface quasi particle model

Let's first evaluate the 2ν DBD NMEs. The half-life $t_{1/2}$ is given by the phase space factor $G^{2\nu}$ and the NME $M^{2\nu}$ as

$$t_{1/2}^{-1} = G^{2\nu} [M^{2\nu}]^2. \quad (1)$$

Here the axial vector weak coupling constant $g_A=1.267$ in unit of the vector one of g_F is conventionally included in $G^{2\nu}$. The $2\nu\beta^-\beta^-$ NME for the $A(Z, N) \rightarrow C(Z+2, N-2)$ ground-state to ground state $0^+ \rightarrow 0^+$ transition is expressed as

$$M^{2\nu} = \sum_i \frac{M_i^- M_i^+}{\Delta_i}, \quad (2)$$

where M_i^- and M_i^+ are GT NMEs for the $\beta^- A(Z, N) \rightarrow B(Z+1, N-1)$ and $\beta^+ C(Z+2, N-2) \rightarrow B(Z+1, N-1)$ transitions via the i th state in the intermediate nucleus $B(Z+1, N-1)$, and Δ_i is the energy denominator [2, 4].

Note that the 2ν NMEs for $2\nu\text{ECEC}$, $2\nu\beta^+\text{EC}$ and $2\nu\beta^+\beta^+$ decays for $A(Z, N) \leftarrow C(Z+2, N-2)$ are expressed by the same eq.(2), but their halfives are deduced from eq.(1) by using their phase space factors.

We discuss mainly DBD NMEs in medium heavy nuclei of current interest. GT strength distributions for the DBD nuclei have been well studied by charge exchange reactions (CER), particularly by the high energy-resolution ($^3\text{He}, t$) reactions, as discussed in the review articles [1, 2, 4]. They show low-lying GT states with weak strength of $B(GT) \approx 0.05-0.3$ and a strong β^- GT giant resonance (GR) with $B(GT) \approx 1.5 (N-Z)$ at the high excitation region of $E=10-15$ MeV. There is no strong β^+ GT GR since β^+ p \rightarrow n GT transitions are blocked by the neutrons in the same shell with the protons in medium heavy nuclei.

In the FSQP model [2, 4, 11, 12], the $2\nu\beta\beta$ NME is expressed as the sum of the NMEs via the intermediate FSQP states. The quasi-particle configurations involved in the transition of $A(0^+) \rightarrow B(1^+) \rightarrow C(0^+)$ are $(J_i J_i)_0 \rightarrow (J_i j_k)_1 \rightarrow (j_k j_k)_0$, where J_i and

j_k are the i neutron and k proton spins. The Fermi surface is diffused due to the pairing interaction. The quasi-particle pairs to be considered are the quasi-neutron pairs of $(J_i J_i)_0$ in the defused Fermi surface of A, and the quasi-proton pairs of $(j_k j_k)$ in the defused Fermi surface of C. Since the quasi-neutron J_i and the quasi-proton j_k are in the 0^+ ground states of A and C, the intermediate states of (J_i, j_k) are necessarily FSQP low-lying states in B within the energy width around the pairing energy of a few MeV.

The FSQP GT NMEs M_i^\pm for β^\pm is simply expressed as [2, 11, 12],

$$M_i^\pm = k^\pm M_i^\pm(QP), \quad M_i^\pm(QP) = P_i^\pm M(J_i j_i), \quad (3)$$

where $M_i^\pm(QP)$ is the quasi-particle NME, k^\pm is the effective axial coupling constant in units of the axial coupling g_A [1, 13] and P_i^\pm is the pairing correlation coefficient for β^\pm transition, and $M(J_i j_i)$ is the single particle $J_i \rightarrow j_i$ GT NME. Here P_i^\pm stands for the reduction coefficient due to the pairing correlations and k^\pm does for the coefficient due to the spin-isospin correlations and nuclear medium effects as discussed before [1, 4, 13], and also recently on the GT and SD β NMEs [14, 15].

The pairing reduction coefficients are given as

$$P^-(Jj) = V_J(N)U_j(Z), \quad P^+(Jj) = U_J(N-2)V_j(Z+2), \quad (4)$$

where $V_J(N)$ and $U_j(Z)$ are the occupation and vacancy coefficients for J quasi-neutron and j quasi-proton orbits in the initial nucleus A, and $V_j(Z+2)$ and $U_J(N-2)$ are those for j quasi-proton and J quasi-neutron in the final nucleus C. Since the same SP NME of $M(J_i j_i)$ is involved in both the M_i^- and M_i^+ , the product is positive, and thus the sum is constructive. The GT NMEs for the FSQP states in the low excitation region are evaluated from the experimental CER and/or the β^\pm rates.

The unique features of the FSQP $M^{2\nu}$ are as follow.

- The $2\nu\beta\beta$ decays are expressed as the successive β^\pm transitions via the low-lying FSQP intermediate states, where the single β^\pm NMEs, including g_A^{eff}/g_A , are given experimentally by CERs and β/EC rates. Thus one does not need to evaluate pure theoretically the nuclear correlations and the effective g_A involved in NMEs, which are very hard. There are no appreciable contributions from the GT giant resonance to $2\nu\beta\beta$ NMEs as evaluated theoretically [16].
- The FSQP M^\pm is smaller than the SP NME by the pairing coefficient $P^\pm \approx 0.45-0.25$ and the effective coupling coefficient $k^\pm \approx 0.3-0.2$. [2, 4, 13]. Thus $M^{2\nu}$ becomes smaller by the coefficient $k^- P^- k^+ P^+ \approx 0.01-0.005$ with respect to the single particle value.
- The values $M^{2\nu}$ reflect the GT β^\pm strength distributions in the intermediate nucleus. They are large in nuclei where a large GT $^\pm$ strength is located at the ground state with a small Δ_1 , as seen in the NMEs for ^{100}Mo ^{106}Cd and ^{110}Pd nuclei
- $M^{2\nu}$ depends on the shell structure as the pairing coefficient P^\pm [11]. The product $P_i^- P_i^+$ of the pairing factors is very stable in the middle of the shell, but gets

small near the shell/sub-shell closure because the the vacancy amplitude U or the occupation amplitude V gets small just before or after the shell closure.

3. Two neutrino DBD NMEs

The $2\beta^-\beta^-$ nuclei to be discussed in the present paper are ^{76}Ge , ^{82}Se , ^{96}Zr ^{100}Mo , ^{110}Pd , ^{116}Cd , ^{128}Te , ^{130}Te , and ^{136}Xe . These are interesting for $0\nu\beta\beta$ studies because of the large phase volume of $G^{0\nu}$. The $2\nu\beta\beta$ halfives for them, except ^{110}Pd , are known experimentally. The observed and evaluated 2ν NMEs are shown in Table 1.

The FSQP NME for ^{76}Ge , ^{82}Se and ^{110}Pd are the present values and the NMEs for ^{136}Xe and others are from the previous works of ref.[12] and ref.[11]. The data for single beta decays and charge exchange reactions [20, 21, 22, 23, 24, 25, 26, 27] are used to evaluate the FSQP NMEs. The present values for ^{76}Ge and ^{82}Se are nearly the same as the previous values [11]. The observed and FSQP NMEs are in good agreement as given in Table 1. The new NME of 0.145 for the ^{110}Pd is quite large. It gives the halflife of $t_{1/2} = 1.3 \cdot 10^{20}$ y. Theoretical pnQRPA values of 1.1-0.91 10^{20} y [28] and 1.2-1.8 10^{20} y [29] and the SSD value of 1.2 10^{20} y [30] are close to the present value. The experimental study with the 10^{20} y sensitivity is encouraged.

The $2\nu\text{ECEC}$, $2\nu\beta^+\text{EC}$ and $2\nu\beta^+\beta^+$ DBDs are not well studied because of the small phase volume. Here we discuss three DBDs of ^{78}Kr , ^{106}Cd , and ^{130}Ba . The experimental and FSQP NMEs are shown in Table 2. The $M^{2\nu}(EXP)$ limits for ^{78}Kr [31] and ^{106}Cd [32] are from the ECEC data and the NME for ^{130}Ba is from geochemical method [19].

DBDs listed in Tables 1 and 2 are classified into three groups as given in Table 3. Group I: FSQP neutrons and protons are in the same $N=3$ major shell. Group II:

Table 1. The $2\nu\beta^-\beta^-$ NMEs for the $0^+ \rightarrow 0^+$ ground state 0^+ and for the first excited 0^+ (*) transitions. $Q_{\beta\beta}$: Q value. $M^{2\nu}(EXP)$: experimental NME with a ref.[17], b ref.[19] and others ref. [11]. $M^{2\nu}(FSQP)$: FSQP NME with c ref.[12], d the present value and others ref.[11].

Transition	$Q_{\beta\beta}$ MeV	$M^{2\nu}(EXP)$	$M^{2\nu}(FSQP)$
$^{76}\text{Ge} \rightarrow ^{76}\text{Se}$	2.039	0.063 ^a	0.052 ^d
$^{82}\text{Se} \rightarrow ^{82}\text{Se}$	2.992	0.050	0.064 ^d
$^{96}\text{Zr} \rightarrow ^{96}\text{Mo}$	3.346	0.049	0.045
$^{100}\text{Mo} \rightarrow ^{100}\text{Mo}$	3.034	0.126	0.096
$^{100}\text{Mo} \rightarrow ^{100}\text{Mo}^*$	1.904	0.102	0.090
$^{110}\text{Pd} \rightarrow ^{110}\text{Cd}$	2.000	-	0.145 ^d
$^{116}\text{Cd} \rightarrow ^{116}\text{Sn}$	2.804	0.070	0.055
$^{128}\text{Te} \rightarrow ^{128}\text{Xe}$	0.867	0.025	0.019
$^{130}\text{Te} \rightarrow ^{130}\text{Xe}$	2.529	0.018	0.017
$^{136}\text{Xe} \rightarrow ^{136}\text{Ba}$	2.467	0.010 ^b	0.012 ^c

Table 2. The 2ν ECEC NME for the $0^+ \rightarrow 0^+$ ground state transition. See the caption of the table 1. a: ref.[31]. b: ref.[32]. c: ref.[19]. d: present value.

Transition	$Q_{\beta\beta}$ MeV	$M^{2\nu}(EXP)$	$M^{2\nu}(FSQP)$
$^{78}\text{Kr} \rightarrow ^{78}\text{Se}$	2.866	$\leq 0.34^a$	0.065^d
$^{106}\text{Cd} \rightarrow ^{106}\text{Pd}$	2.770	$\leq 0.39^b$	0.11^d
$^{130}\text{Ba} \rightarrow ^{130}\text{Xe}$	2.610	0.105^c	0.067^d

ESQP protons and neutrons are in the $N=3$ and $N=4$ major shells, respectively. Group III: FSQP neutrons and protons are in the same $N=4$ major shell. Group I: ^{76}Ge , ^{78}Kr , ^{82}Se . Group II: ^{96}Zr , ^{100}Mo , ^{106}Cd , ^{110}Pd , ^{116}Cd . Group III: ^{128}Te , ^{130}Te , ^{130}Ba , ^{136}Xe .

Table 3. FSQP shell configurations for the three groups (G) of the DBD nuclei.

G	Z, N	FSQP GT configurations
I	$32 \leq Z \leq 36, 42 \leq N \leq 48$	$1g_{9/2}^p 1g_{9/2}^n, 1f_{5/2}^p 1f_{5/2}^n, 2p_{3/2}^p 2p_{1/2}^n$
II	$40 \leq Z \leq 48, 56 \leq N \leq 68$	$1g_{9/2}^p 1g_{7/2}^n$
III	$52 \leq Z \leq 56, 76 \leq N \leq 82$	$2d_{5/2}^p 2d_{3/2}^n, 1h_{11/2}^p 1h_{11/2}^n, 3s_{1/2}^p 3s_{1/2}^n$

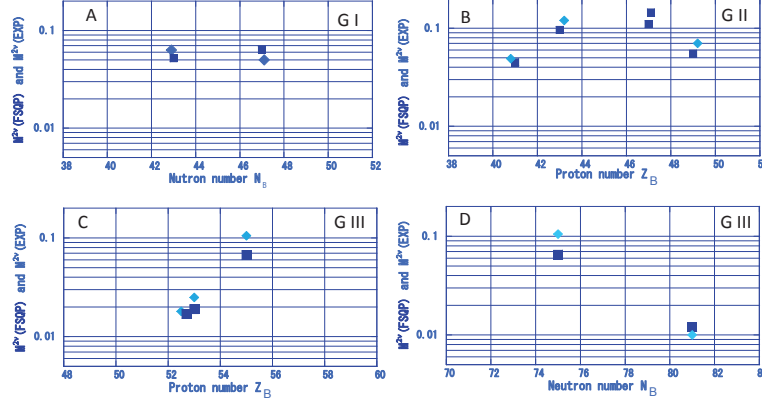
All FSQP states in the low excitation region are involved more or less in the 2ν DBD. In case of the group II nuclei, the FSQP protons and neutrons are in different major shells, and the ground state is the only one strong GT state of $1g_{9/2}^p 1g_{7/2}^n$ in the low-excitation region, as observed in the ($^3\text{He}, t$) CERs [33, 34, 35, 36]. Thus the hypothesis of the single state dominance (SSDM) [37] is valid only for nuclei in this group. In cases of the Group I and III nuclei, the FSQP protons and neutrons are in the same major shell. Thus there are several FSQP states in the low excitation region of the intermediate nucleus [33, 34, 35, 36], and they all contribute to $M^{2\nu}$.

The experimental and FSQP 2ν NMEs are shown as a function of the proton and neutron numbers of the intermediate nuclei in Fig.1. They show clearly similar sub-shell structures. The NMEs for group II nuclei get small at the opening of $Z=40$ and the closure of $Z=50$ for the $g_{9/2}$ proton shell, and get large in the middle (Fig.1.B). The NMEs for the group III get small as the proton number approaches to the shell closure of $Z=50$ (Fig.1 C) and as the neutron number to that of $N=82$ (Fig.1.D).

These simple systematic features of the FSQP model are different from the QRPA calculations [38, 39]. The small NMEs $M^{2\nu}$ are attributed to the cancellation of the amplitudes in the QRPA β NMEs at a certain value of g_{pp} (particle particle interaction). In other words, the QRPA calculations reproduce the experimental $M^{2\nu}$ values by adjusting g_{pp} and g_A . On the other hand, FSQP is based on the experimental single β^\pm NMEs for the low lying states, but not on any adjustable parameters.

ECEC, $\text{EC}\beta^+$ and $\beta^+\beta^+$ DBDs are not well studied experimentally because their phase space factors are rather small. The evaluated halfives on the basis of the FSQP

Figure 1. The FSQP and experimental NMEs of $M^{2\nu}(FSQP)$ (squares) and $M^{2\nu}(EXP)$ (diamonds) for nuclei in the group I (A) and II (B) and III (C and D). Z_B and N_B are the proton and neutron numbers in the intermediate nucleus.



NMEs are shown in Table 4. The experimental limit of $5.5 \cdot 10^{21}$ y [31] for the ^{78}Kr KK life is smaller than the FSQP value by a factor around 20, while the limits of $2.7 \cdot 10^{20}$ y [40] and $4.2 \cdot 10^{20}$ [32] for the ^{106}Cd ECEC are a factor around 15 smaller than the FSQP value. The limit of $1.1 \cdot 10^{21}$ [41] for $2\nu\beta^+\text{EC}$ is also smaller than the FSQP by a factor 20. On the other hand, the half-life of $2.2 \cdot 10^{21}$ y for ^{130}Ba [10] derived by a geochemical method is close to the FSQP life, but shorter a little than it.

Theoretical half-lives do depend on the models and the parameters used for the calculations. $2\nu\text{ECEC}$ half-lives of $3.7 \cdot 10^{21}$ - $9.4 \cdot 10^{22}$ y for ^{78}Kr [42, 43, 45] are shorter than the FSQP values. The values for ^{106}Cd ECEC half-lives are 0.12 - $5.5 \cdot 10^{21}$ y by QRPA/RQRPA/SQRPA [44, 45, 46], 9.7 - $25 \cdot 10^{21}$ y by PHFB [47] and 1.7 - $4.2 \cdot 10^{21}$ y by SU(4) [48]. The $2\nu\text{ECEC}$ half-life for ^{130}Ba by QRPA [42] is $4.2 \cdot 10^{21}$ y. On the other hand, the SSDH gives $\leq 1.6 \cdot 10^{24}$ y, $\geq 4.4 \cdot 10^{21}$ y and $5.0 \cdot 10^{22}$ y for the $2\nu\text{ECEC}$ half-lives of ^{78}Kr , ^{106}Cd , and ^{130}Ba [30]. The SSDH values for ^{78}Kr and ^{130}Ba in the group I and III are much longer than the FSQP ones because the calculation does not include the excited FSQP states.

Table 4. FSQP NMEs and half-lives for the 2ν DBDs of ^{78}Kr , ^{106}Cd and ^{130}Ba . $G^{2\nu}$: phase space factor from ref. [6].

Decay mode	^{78}Kr	^{106}Cd	^{130}Ba
$M^{2\nu}$	0.065	0.11	0.067
ECEC	$1.2 \cdot 10^{23}$	$5.2 \cdot 10^{21}$	$5.4 \cdot 10^{21}$
$\text{EC}\beta^+$	$2.0 \cdot 10^{23}$	$4.1 \cdot 10^{22}$	$1.6 \cdot 10^{23}$
$\beta^+\beta^+$	$7.0 \cdot 10^{26}$	$1.7 \cdot 10^{27}$	$1.9 \cdot 10^{29}$

4. Remarks and discussions

Now, we discuss impact of the present discussions on the the $0\nu\beta\beta$ NMEs $M^{0\nu}$. It has been believed long that i $M^{2\nu}$ is very small because it is sensitive to g_{pp} and the amplitudes involved in $M^{2\nu}$ cancels at the appropriate value of g_{pp} , while $M^{0\nu}$ is large because it is not sensitive to g_{pp} and ii $M^{0\nu}$ includes several multipole NMEs and it is not sensitive to the individual nuclear structures, and thus they are considered to be nearly the same for all nuclei.

On the other hand, the FSQP model shows that $M^{2\nu}$ is much smaller than the quasi-particle NME M_{QP} by the reduction coefficient $(k^\pm)^2 \approx 0.05-0.1$ because the observed single β^\pm GT(1^+) M^\pm is smaller than the single quasi-particle M_{QP}^\pm (GT) by the coefficient $k^\pm = k^{eff} \approx 0.2-0.3$. The single β^\pm SD(2^-) M^\pm , which is one of the major components of $M^{0\nu}$, is smaller than the single quasi-particle M_{QP}^\pm (SD) by the coefficient $k^{eff} \approx 0.2-0.3$ [15], as in case of the GT NME [14]. Accordingly, the axial-vector component of $M^{0\nu}$ may be much smaller than the QP NME $M_{QP}^{0\nu}$ by the coefficient $(k^{eff})^2 \approx 0.05-0.1$.

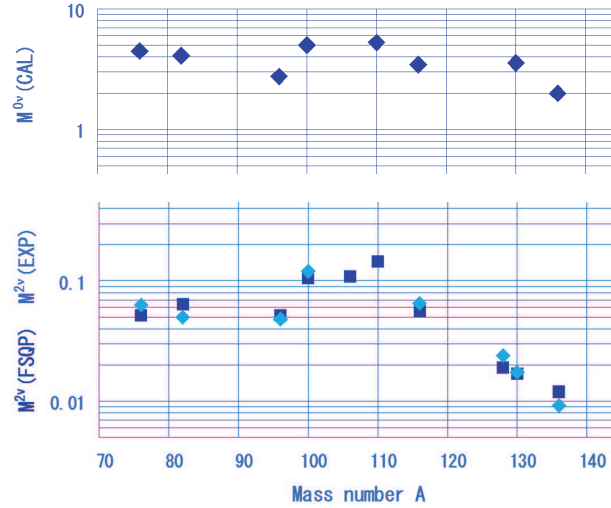
The reduction coefficient is given as $k^{eff} = k_{\tau\sigma} \times k_{NM}$, where $k_{\tau\sigma} \approx 0.4 - 0.6$ and $k_{NM} \approx 0.4 - 0.6$ stand for the nucleonic $\tau\sigma$ correlation and and the non-nucleonic nuclear medium effects [15, 14]. The former is incorporated in pnQRPA with the nucleonic $\tau\sigma$ correlations, while the latter may be expressed in terms of the effective g_A^{eff}/g_A^{free} . Actually, the values of $g_A^{eff}/g_A^{free} \approx 0.5 - 0.7$ are used in recent theoretical calculations such as shell model [49, 50], pnQRPA [51, 52], and IBA2 [53]. Then $M^{0\nu}$ may be reduced with respect to the pnQRPA NME by a factor 2-3, depending on the higher multi-pole axial vector NMEs and the vector NMEs.

In the present cases of the ground-state to ground state DBDs, the values for $M^{0\nu}$ near closed and sub-closed shells may get small due to the pairing factor P^\pm as in cases of $M^{2\nu}$. Then both $M^{0\nu}$ and $M^{2\nu}$ for ^{136}Xe are small due to the small paring factor P^+ near the neutron closed shell at 82. Thus the $0\nu\beta\beta$ signal rate may get small due to the small $M^{0\nu}$, but the BG contribution from the high energy tail of the $2\nu\beta\beta$ spectrum to the $0\nu\beta\beta$ peak region gets small also in case of modest energy-resolution experiments.

The $0\nu\beta\beta$ NMEs have been calculated on various nuclei. The averaged value [5] for each DBD isotope of the current interest is plotted in fig.2. The $0\nu\beta\beta$ NMEs do show the similar dependence on the shell configuration as $2\nu\beta\beta$ NME. The $0\nu\beta\beta$ NMEs get small near the sub closed shell due to the small U or V coefficients as in case of the $2\nu\beta\beta$ NMEs. This is in contrast to the general belief that all the $0\nu\beta\beta$ NMEs are large and same. Then, one may need to consider small and structure-dependent NMEs $M^{0\nu}$ as well in selecting DBD nuclei to be studied in future DBD experiments.

Experimental studies of $2\nu\text{ECEC}$ of ^{78}Kr , ^{106}Cd , ^{110}Pd , and ^{130}Ba are encouraged to verify the FSQP prediction. The single β^\pm NMEs for 3^+ and 4^- transitions in DBD nuclei are interesting to check if similar reductions of the NMEs as GT and SD are seen for higher multipole NMEs as well.

Figure 2. Top: Average values for the calculated NMEs $M^{0\nu}$ [5]. Bottom: The FSQP NMEs $M^{2\nu}(FSQP)$ (squares) and experimental NMEs $M^{2\nu}(EXP)$ (diamonds) for $\beta^-\beta^-$ DBDs.



The authors thank Prof. D. Frekers and Prof. J. Suhonen for valuable discussions.

5. References

- [1] H. Ejiri 2000 *Phys. Rep.* **338** 265
- [2] H. Ejiri 2005 *J. Phys. Soc. Jpn.* **74** 2101
- [3] F. Avignone, S. Elliott and J. Engel 2008 *Rev. Mod. Phys.* **80** 481
- [4] J. Vergados, H. Ejiri, F. Šimkovic 2012 *Rep. Prog. Phys.* **75** 106301
- [5] J. Vergados, H. Ejiri, F. Šimkovic 2012 *Int. J. Modern Physics E* **25** 1630007
- [6] J. Suhonen, O. Civitarese 1998 *Phys. Rep.* **300** 123
- [7] A. Faessler *et al.* 2008 *J. Phys. G* **35** 075104
- [8] J. Suhonen, O. Civitarese 2012 *J. Phys. G: Nucl. Part. Phys.* **39** 124005
- [9] J. Suhonen, O. Civitarese 2012 *J. Phys. G: Nucl. Part. Phys.* **39** 085105
- [10] A.P. Meshik *et al.* 2001 *Phys. Rev. C*, **64** 035205
- [11] H. Ejiri 2009 *J. Phys. Soc. Jpn.* **78** 074201
- [12] H. Ejiri 2012 *J. Phys. Soc. Jpn. letters.* **81** 033201
- [13] H. Ejiri and J.I. Fujita 1978 *Phys. Rep. C* **38** 85
- [14] H. Ejiri and J. Suhonen 2015 *J. Phys. G* **42** 055201
- [15] H. Ejiri, N. Soukouti, J. Suhonen 2014 *Phys. Lett. B* **729** 27
- [16] H. Ejiri and H. Toki 1995 *J. Phys. Soc. Japan* **65** 7
- [17] M. Agostini *et al.*, 2015 *Eur. Phys. J. C* **75** 416.
- [18] J.B. Albert *et al.*, 2014 *Phys. Rev. D* **90** 092004.
- [19] A. Barabash 2010 *Phys. Rev. C* **81** 035501.
- [20] R.B. Firestone, *et al.* 1999 *Table of Isotopes, 8th ed., LBL*
- [21] ENSDF at NNDC site <http://www.nndc.bnl.gov/>
- [22] D. De Fyenne and A. Negret 2008 *Nucl. Data Sheets* **109** 943
- [23] D. De Frenne and E. Jacabs 1996 *Nucl. Data Sheets* **79** 639
- [24] J. Blachat 2000 *Nucl. Data Sheets* **90** 135
- [25] J. Blachat 2012 *Nucl. Data Sheets* **113** 515

- [26] J. Blachot 2010 *Nucl. Data Sheets* **111** 717
- [27] G. Gürdal and F.G. Kondev 2012 *Nucl. Data Sheets* **113** 1315
- [28] J. Suhonen 2011 *Nucl. Phys. A* **864** 63
- [29] O. Civitarese and J. Suhonen 1998 *Phys. Rev. C* **58** 1535
- [30] P. Domin et al., 2005 *Nuclear Physics A* **753** 337
- [31] Ju. M. Gavriljuk et al. 2013 *Phys. Rev. C* **87** 035501
- [32] N.I. Rukhadze, TGV collaboration, 2015 *Proc. MEDEX15, APS Conf. Proc.* **1686** 020020; 2011 *Bull. Russ. Acad. Sci. Phys.* **75** 879; 2011 *Nucl. Phys. A* **852** 197
- [33] H. Akimune et al. 1997 *Phys. Lett., B* **394** 23
- [34] J. H. Thies et al. 2012 *Phys. Rev. C*, **86** 014304
- [35] P. Puppe et al. 2011 *Phys. Rev. C*, **84** 051305(R)
- [36] P. Puppe et al. 2012 *Phys. Rev. C*, **86** 044603
- [37] J. Abad et al., 1984 *Ann. fis. A* **80** 9
- [38] P. Vogel, M.R. Zirnbauer 1986 *Phys. Rev. Lett.* **57** 3148
- [39] V. A. Rodin, A. Faessler, F. Šimkovic and P. Vogel 2006 *Nucl. Phys. A* **766** 107, 2007 *A793* 213(E)
- [40] F. Danevich, 2015 *Proc. MEDEX15, APS Conf. Proc.* **1686** 020006
- [41] P. Bell et al. 2016 *Phys. Rev. C* **93** 045502
- [42] M. Hirsh et al. 1994 *Z. Physik A* **347** 151
- [43] M. Aunola and J. Suhonen 1996 *Nuclear Physics A* **602** 133
- [44] J. Suhonen and O. Civitarese 2001 *Phys. Lett. B* **497** 221
- [45] J. Toivanen and J. Suhonen 1997 *Phys. Rev. C* **55** 2314
- [46] S. Stoica and H.V. Klapdor-Kleingrothaus 2003 *Eur. J. Phys. A* **17** 529
- [47] A. Shukla et al. 2005 *Eur. J. Phys. A* **23** 235
- [48] O. A. Ramyantsev and M. H. Uhrin. 1998 *Phys. Lett. B* **443** 51
- [49] G. Martínez-Pinedo, A. Poves, E. Caurier, A.P. Zuker 1996 *Phys. Rev. C* **53** R2602
- [50] E. Caurier, F. Nowachi and A. Poves 2012 *Physics Letters B* **711** 62
- [51] J. Suhonen, O. Civitarese 2013 *Phys. Lett. B* **725** 153
- [52] J. Suhonen, O. Civitarese, 2014 *Nucl. Phys. A* **924** 1
- [53] J. Barea, J. Kotila, F. Iachello 2013 *Phys. Rev. C* **87** 014315